
FiLM: Frequency improved Legendre Memory Model for Long-term Time Series Forecasting

Abstract

Recent studies have shown that deep learning models such as RNNs and Transformers have brought significant performance gains for long-term forecasting of time series because they effectively utilize historical information. We found, however, that there is still great room for improvement in how to preserve historical information in neural networks while avoiding overfitting to noise presented in the history. Addressing this allows better utilization of the capabilities of deep learning models. To this end, we design a Frequency improved Legendre Memory model, or **FiLM**: it applies Legendre Polynomials projections to approximate historical information, uses Fourier projection to remove noise, and adds a low-rank approximation to speed up computation. Our empirical studies show that the proposed FiLM significantly improves the accuracy of state-of-the-art models in multivariate and univariate long-term forecasting by **(20.3%, 22.6%)**, respectively. We also demonstrate that the representation module developed in this work can be used as a general plug-in to improve the long-term prediction performance of other deep learning modules. Code will be released soon.

1 Introduction

Long-term forecasting refers to making predictions based on the history for a long horizon in the future, as opposed to short-term forecasting. Long-term time series forecasting has many key applications in energy, weather, economics, transportation, and so on. It is more challenging than ordinary time series forecasting. Some of the challenges in long-term forecasting include long-term time dependencies, susceptibility to error propagation, complex patterns, and nonlinear dynamics. These challenges make accurate predictions generally impossible for traditional learning methods such as ARIMA. Although RNN-like deep learning methods have made breakthroughs in time series forecasting [Rangapuram et al. \(2018\)](#); [Salinas et al. \(2020\)](#), they often suffer from problems such as gradient vanishing/exploding [Pascanu et al. \(2013\)](#), which limits their practical performance. Following the success of Transformer [Vaswani et al. \(2017\)](#) in the NLP and CV communities [Vaswani et al. \(2017\)](#); [Devlin et al. \(2019\)](#); [Dosovitskiy et al. \(2021\)](#); [Rao et al. \(2021\)](#), it also shows promising performance in capturing long-term dependencies [Zhou et al. \(2021\)](#); [Wu et al. \(2021\)](#); [Zhou et al. \(2022\)](#); [Wen et al. \(2022\)](#) for time series forecasting. We provide an overview of this line of work (including deep recurrent networks and efficient Transformers) in the appendix A.

In order to achieve accurate predictions, many deep learning researchers increase the complexity of their models, hoping that they can capture critical and intricate historical information. These methods, however, cannot achieve it. Figure 1 compares the ground truth time series of the real-world ETTm1 dataset with the predictions of the vanilla Transformer method and the LSTM model [Vaswani et al. \(2017\)](#); [Hochreiter & Schmidhuber \(1997a\)](#) [Zhou et al. \(2021\)](#). It is observed that the prediction is completely off from the distribution of the ground truth. We believe that such errors come from these models miscapturing noise while attempting to preserve the true signals. We conclude that two keys in accurate forecasting are: 1) how to capture critical historical information as complete as possible; and 2) how to effectively remove the noise. Therefore, to avoid a derailed

forecast, we cannot improve a model by simply making it more complex. Instead, we shall consider a robust representation of the time series that can capture its important patterns without noise.

This observation motivates us to switch our view from long-term time series forecasting to long-term sequence compression. Recursive memory model [Voelker et al. \(2019\)](#); [Gu et al. \(2021a,b, 2020\)](#) has achieved impressive results in function approximation

tasks. [Voelker et al. \(2019\)](#) designed a recursive memory unit (LMU) using Legendre projection, which provides a good representation for long time series. *S4* model [Gu et al. \(2021a\)](#) comes up with another recursive memory design for data representation and significantly improves state-of-the-art results for Long-range forecasting benchmark (LRA) [Tay et al. \(2020b\)](#). However, when coming to long-term time series forecasting, these approaches fall short of the Transformer-based methods' state-of-the-art performance. A careful examination reveals that these data compression methods are powerful in recovering the details of historical data compared to LSTM/Transformer models, as revealed in Figure 2. However, they are vulnerable to noisy signals as they tend to overfit all the spikes in the past, leading to limited long-term forecasting performance. It is worth noting that, Legendre Polynomials employed in LMP [Voelker et al. \(2019\)](#) is just a special case in the family of Orthogonal Polynomials (OPs). OPs (including Legendre, Laguerre, Chebyshev, etc.) and other orthogonal basis (Fourier and Multiwavelets) are widely studied in numerous fields and recently brought in deep learning [Wang et al. \(2018\)](#); [Gupta et al. \(2021\)](#); [Zhou et al. \(2022\)](#); [Voelker et al. \(2019\)](#); [Gu et al. \(2020\)](#). A detailed review can be found in Appendix A.

The above observation inspires us to develop methods for accurate and robust representations of time series data for future forecasting, especially long-term forecasting. The proposed method significantly outperforms existing long-term forecasting methods on multiple benchmark datasets by integrating those representations with powerful prediction models.

As the first step towards this goal, we directly exploit the Legendre projection, which is used by LMU [Voelker et al. \(2019\)](#) to update the representation of time series with fixed-size vectors dynamically. This projection layer will then be combined with different deep learning modules to boost forecasting performance. The main challenge with directly using this representation is the dilemma between information preservation and data overfitting, i.e., the larger the number of Legendre projections is, the more the historical data is preserved, but the more likely noisy data will be overfitted. Hence, as a second step, to reduce the impact of noisy signals on the Legendre projection, we introduce a layer of dimension reduction by a combination of Fourier analysis and low-rank matrix approximation. More specifically, we keep a large dimension representation from the Legendre projection to ensure that all the important details of historical data are preserved. We then apply a combination of Fourier analysis and low-rank approximation to keep the part of the representation related to low-frequency Fourier components and the top eigenspace to remove the impact of noises. Thus, we can not only capture the long-term time dependencies, but also effectively reduce the noise in long-term forecasting. We refer to the proposed method as **Frequency improved Legendre Memory model**, or **FiLM** for short, for long-term time series forecasting.

In short, we summarize the key contributions of this work as follows:

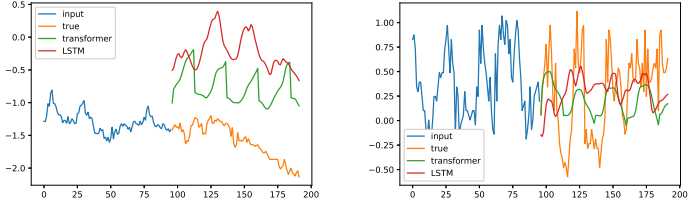


Figure 1: The discrepancy between ground truth and forecasting output from vanilla Transformer and LSTM on a real-world ETT1 dataset Left: trend shift. Right: seasonal shift.

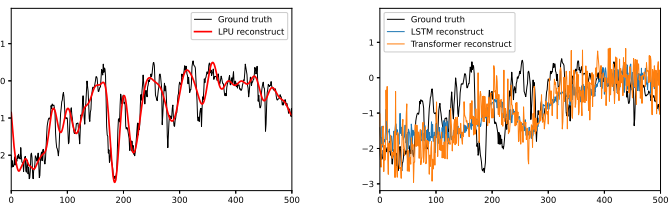


Figure 2: Data recovery with Autoencoder structure: recovery a 1024-length data with a bottleneck of 128 parameters. Left: Legendre Projection Unit. Right: LSTM and vanilla Transformer.

1. We propose a *Frequency improved Legendre Memory model (FiLM)* architecture with a mixture of experts for robust multiscale time series feature extraction.
2. We redesign the *Legendre Projection Unit (LPU)* and make it a general tool for data representation that any time series forecasting model can exploit to solve the historical information preserving problem.
3. We propose *Frequency Enhanced Layers (FEL)* that reduce dimensionality by a combination of Fourier analysis and low-rank matrix approximation to minimize the impact of noisy signals from time series and ease the overfitting problem. The effectiveness of this method is verified both theoretically and empirically.
4. We conduct extensive experiments on six benchmark datasets across multiple domains (energy, traffic, economics, weather, and disease). Our empirical studies show that the proposed model improves the performance of state-of-the-art methods by **19.2%** and **26.1%** in multivariate and univariate forecasting, respectively. In addition, our empirical studies also reveal a dramatic improvement in computational efficiency through dimensionality reduction.

2 Time Series Representation in Legendre-Fourier Domain

2.1 Legendre Projection

Given an input sequence, the function approximation problem aims to approximate the cumulative history at every time t . Using Legendre Polynomials projection, we can project a prolonged sequence of data onto a subspace of bounded dimension, leading to compression, or feature representation, for evolving historical data. Formally, given a smooth function f observed online, we aim to maintain a fixed size compressed representation of its history $f(x)_{[t-\theta, t]}$, where θ specifies the window size. At every time point t , the approximation function $g^{(t)}(x)$ is defined with respect to the measure $\mu^{(t)} = \frac{1}{\theta} \mathbb{I}_{[t-\theta, t]}(x)$. In this paper, we use Legendre Polynomials of degree at most $N - 1$ to build the function $g^{(t)}(x)$, i.e.

$$g^{(t)}(x) = \sum_{n=1}^N c_n(t) P_n \left(\frac{2(x-t)}{\theta} + 1 \right), \quad (1)$$

where $P_n(\cdot)$ is the n -th order Legendre Polynomials. Coefficients $c_n(t)$ are captured by the following dynamic equation:

$$\frac{d}{dt} c(t) = -\frac{1}{\theta} A c(t) + \frac{1}{\theta} B f(t). \quad (2)$$

where the definition of A and B can be found in [Voelker et al. \(2019\)](#). Using Legendre Polynomials as a basis allows us to accurately approximate smooth functions, as indicated by the following theorem.

Theorem 1 (*Similar to Proposition 6 in [Gu et al. \(2020\)](#)*). *If $f(x)$ is L -Lipschitz, then $\|f_{[t-\theta, t]}(x) - g^{(t)}(x)\|_{\mu^{(t)}} \leq \mathcal{O}(\theta L / \sqrt{N})$. Moreover, if $f(x)$ has k -th order bounded derivatives, we have $\|f_{[t-\theta, t]}(x) - g^{(t)}(x)\|_{\mu^{(t)}} \leq \mathcal{O}(\theta^k N^{-k+1/2})$.*

According to Theorem 1, without any surprise, the larger the number of Legendre Polynomials basis, the more accurate the approximation will be, which unfortunately may lead to the overfitting of noisy signals in the history. As shown in Section 4, directly feeding deep learning modules, such as MLP, RNN, and vanilla Attention without modification, with the above features will not yield state-of-the-art performance, primarily due to the noisy signals in history. That is why we introduce, in the following subsection, a Frequency Enhanced Layer with Fourier transforms for feature selection.

Before we close this subsection, we note that unlike [Gu et al. \(2021a\)](#), a fixed window size is used for function approximation and feature extraction. This is largely because a longer history of data may lead to a larger accumulation of noises from history. To make it precise, we consider an auto-regressive setting with random noise. Let $\{x_t\} \in \mathbb{R}^d$ be the time sequence with $x_{t+1} = Ax_t + b + \epsilon_t$ for $t = 1, 2, \dots$, where $A \in \mathbb{R}^{d \times d}$, $b \in \mathbb{R}^d$, and $\epsilon_t \in \mathbb{R}^d$ is random noise sampled from $N(0, \sigma^2 I)$. As indicated by the following theorem, given x_t , the noise will accumulate in $x_{t-\theta}$ over time at the rate of $\sqrt{\theta}$, where θ is the window size.

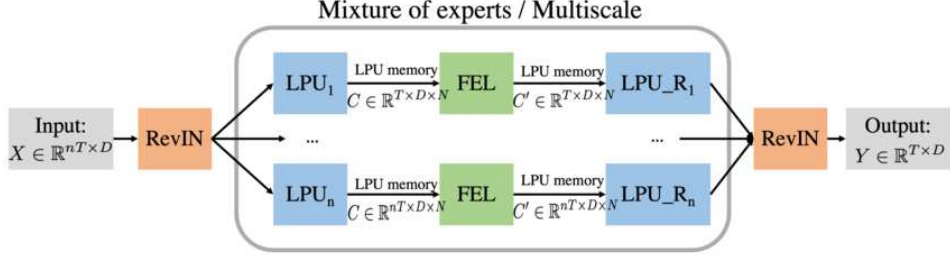


Figure 3: Overall structure of FiLM (Frequency improved Legendre Memory Model). LPU: Legendre Projection Unit. LPU_R: reverse recovery of Legendre Projection. FEL: Frequency Enhanced Layer. RevIn: data normalization block. The input data is first normalized and then project to Legendre Polynomials space (LPU memory C). The LPU memory C is processed with FEL and generates the memory C' of output. Finally, C' is reconstructed and denormalized to output series with LPU_R. A multiscale structure is employed to process the input with length $\{T, 2T, \dots nT\}$.

Theorem 2. Let A be an unitary matrix and ϵ_t be σ^2 -subgaussian random noise. We have $x_t = A^\theta x_{t-\theta} + \sum_{i=1}^{\theta-1} A^i b + \mathcal{O}(\sigma\sqrt{\theta})$.

2.2 Fourier Transform

Because white noise has a completely flat power spectrum, it is commonly believed that the time series data enjoys a particular spectral bias, which is not generally randomly distributed in the whole spectrum. Due to the stochastic transition environment, the real output trajectories of the forecasting task contain large volatilities and people usually only predict the mean path of them. The relative more smooth solutions thus are preferred. According to Eq. (1), the approximation function $g^{(t)}(x)$ can be stabilized via smoothing the coefficients $c_n(t)$ in both t and n . This observation helps us design an efficient data-driven way to tune the coefficients $c_n(t)$. As smoothing in n can be simply implemented via multiplying learnable scalars to each channel, we mainly discuss smoothing $c_n(t)$ in t via Fourier transformation. The spectral bias implies the the spectrum of $c_n(t)$ mainly locates in low frequency regime and has weak signal strength in high frequency regime. To simplify our analysis, let us assume the Fourier coefficients of $c_n(t)$ as $a_n(t)$. Per spectral bias, we assume that there exists a $s, a_{\min} > 0$, such that for all n we have $t > s, |a_n(t)| \leq a_{\min}$. An idea to sample coefficients is to keep the the first k dimensions and randomly sample the remaining dimensions instead of the fully random sampling strategy. We characterize the approximation quality via the following theorem:

Theorem 3. Let $A \in \mathbb{R}^{d \times n}$ be the Fourier coefficients matrix of an input matrix $X \in \mathbb{R}^{d \times n}$, and $\mu(A)$, the coherence measure of matrix A , is $\Omega(k/n)$. We assume there exist s and a positive a_{\min} such that the elements in last $d - s$ columns of A is smaller than a_{\min} . If we keep first s columns selected and randomly choose $\mathcal{O}(k^2/\epsilon^2 - s)$ columns from the remaining parts, with high probability

$$\|A - P(A)\|_F \leq \mathcal{O} \left[(1 + \epsilon) a_{\min} \cdot \sqrt{(n - s)d} \right],$$

where $P(A)$ denotes the matrix projecting A onto the column selected column space.

Theorem 3 implies that when a_{\min} is small enough, the selected space can be considered as almost the same as the original one.

3 Model Structure

3.1 FiLM: Frequency improved Legendre Memory Model

The overall structure of FiLM is shown in Figure 3. The FiLM maps a sequence $X \mapsto Y$, where $X, Y \in \mathbb{R}^{T \times D}$, by mainly utilizing two sub-layers: Legendre Projection Unit (LPU) layer and Fourier Enhanced Layer (FEL). In addition, to capture history information at different scales, a mixture of experts at different scales is implemented in the LPU layer. An optional add-on data normalization layer RevIN [Kim et al. \(2021\)](#) is introduced to further enhance the model's robustness. It is worth mentioning that FiLM is a simple model with only one layer of LPU and one layer of FEL.

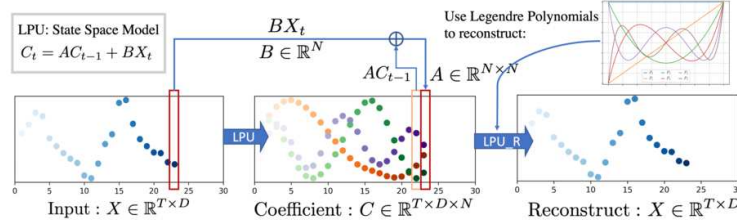


Figure 4: Structure of Legendre Projection Layer (LPU). LPU contains two states: Projection & Reconstruction. $C(t)$ is the compressed memory for historical input up to time t . $x(t)$ is the original input signal at time t . A, B are two pre-fixed projection matrices. $C(t)$ is reconstructed to original input by multiplying a discrete Legendre Polynomials matrix.

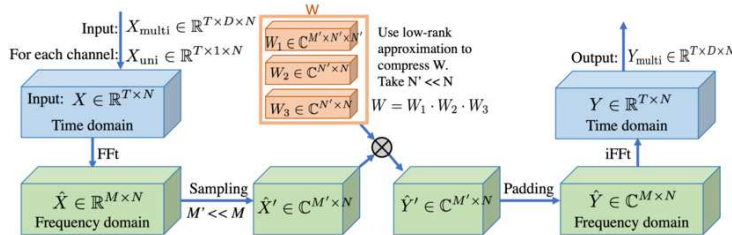


Figure 5: Structure of Frequency Enhanced Layer (FEL): Original version (use weights W) and Low-rank Approximation version (use weights $W = W_1 \cdot W_2 \cdot W_3$), where N is Legendre Polynomials number, M is Fourier mode number, and T is sequence length.

LPU: Legendre Projection Unit LPU is a state space model: $C_t = AC_{t-1} + BX_t$, where $x_t \in \mathbb{R}$ is the input signal, $C_t \in \mathbb{R}^N$ is the memory unit, and N is the number of Legendre Polynomials. LPU contains two untrainable prefixed matrices A and B defined as follows:

$$A_{nk} = (2n+1) \begin{cases} (-1)^{n-k} & \text{if } k \leq n \\ 1 & \text{if } k \geq n \end{cases}, B_n = (2n+1)(-1)^n. \quad (3)$$

LPU contains two stages, i.e., Projection and Reconstruction. The former stage projects the original signal to the memory unit: $C = \text{LPU}(X)$. The later stage reconstructs the signal from the memory unit: $X_{re} = \text{LPU_R}(C)$. The whole process in which the input signal is projected/reconstructed to/from memory C is shown in Figure 4.

FEL: Frequency Enhanced Layer

Low-rank Approximation The FEL is with a single learnable weight matrix ($W \in \mathbb{R}^{M' \times N \times N}$) which is all we need to learn from the data. However, this weight could be large. We can decompose W into three matrices $W_1 \in \mathbb{R}^{M' \times N' \times N'}$, $W_2 \in \mathbb{R}^{N' \times N}$ and $W_3 \in \mathbb{R}^{N' \times N}$ to perform a low-rank approximation ($N' \ll N$). Take Legendre Polynomials number $N = 256$ as default, our model’s learnable weight can be significantly reduced to **0.4%** with $N' = 4$ with minor accuracy deterioration as shown in Section 4. The calculation mechanism is described in Figure 5.

Mode Selection A subset of the frequency modes is selected after Fourier transforms to reduce the noise and boost the training speed. Our default selection policy is choosing the lowest M mode. Various selection policies are studied in the experiment section. Results show that adding some random high-frequency modes can give extra improvement in some datasets, as supported by our theoretical studies in Theorem 3.

Implementation source code for LPU and FEL are given in Appendix B.

3.2 Mixture of Multiscale Experts Mechanism

Multiscale phenomena is a unique critical data bias for time series forecasting. Since we treat history sequence points with uniform importance, our model might lack such prior. Our model implemented a simple mixture of experts strategy that utilizes the input sequence with various time

horizons $\{T, 2T, \dots, nT\}$ to forecast the predicted horizon T and merge each expert prediction with linear layer as shown in Figure 3. This mechanism improves the model's performance consistently across all datasets, as shown in Table 7.

3.3 Data Normalization

As Wu et al. (2021); Zhou et al. (2022) point out, time series seasonal-trend decomposition is a crucial data normalization design for long-term time series forecasting. We find that our LMU projection can inherently play a normalization role for most datasets, but lacking an explicate normalization design still hurt the robustness of performance in some cases. A simple reversible instance normalization (RevIN) Kim et al. (2021) is adapted to act as an add-on explicate data normalization block. The mean and standard deviation are computed for every instance $x_k^{(i)} \in \mathbb{R}^T$ of the input data as $\mathbb{E}_t[x_{kt}^{(i)}] = \frac{1}{T} \sum_{j=1}^T x_{kj}^{(i)}$ and $\text{Var}[x_{kt}^{(i)}] = \frac{1}{T} \sum_{j=1}^T (x_{kj}^{(i)} - \mathbb{E}_t[x_{kt}^{(i)}])^2$. Using these statistics, we normalize the input data $x^{(i)}$ as $\hat{x}_{kt}^{(i)} = \gamma_k \left(\frac{x_{kt}^{(i)} - \mathbb{E}_t[x_{kt}^{(i)}]}{\sqrt{\text{Var}[x_{kt}^{(i)}] + \epsilon}} \right) + \beta_k$, where $\gamma, \beta \in \mathbb{R}^K$ are learnable affine parameter vectors. Then the normalized input data is sent into the model for forecasting. In the end, we denormalize the model output by applying the reciprocal of the normalization performed at the beginning.

RevIN slows down the training process by 2-5 times, and we do not observe consistent improvement on all datasets by applying RevIn. Thus, it can be considered an optional stabilizer in model training. Its detailed performance is shown in the ablation study in Table 7.

4 Experiments

Table 1: multivariate long-term series forecasting results on six datasets with input length $I = 96$ and prediction length $O \in \{96, 192, 336, 720\}$ (For ILI dataset, we use input length $I = 36$ and prediction length $O \in \{24, 36, 48, 60\}$). A lower MSE indicates better performance. All experiments are repeated 5 times.

Methods	FiLM		FEDformer		Autoformer		S4		Informer		LogTrans		Reformer		
Metric	MSE	MAE	MSE	MAE	MSE	MAE	MSE	MAE	MSE	MAE	MSE	MAE	MSE	MAE	
ETTM2	96	0.165	0.256	0.203	0.287	0.255	0.339	0.705	0.690	0.365	0.453	0.768	0.642	0.658	0.619
	192	0.222	0.296	0.269	0.328	0.281	0.340	0.924	0.692	0.533	0.563	0.989	0.757	1.078	0.827
	336	0.277	0.333	0.325	0.366	0.339	0.372	1.364	0.877	1.363	0.887	1.334	0.872	1.549	0.972
	720	0.371	0.389	0.421	0.415	0.422	0.419	0.877	1.074	3.379	1.338	3.048	1.328	2.631	1.242
Electricity	96	0.154	0.267	0.183	0.297	0.201	0.317	0.304	0.405	0.274	0.368	0.258	0.357	0.312	0.402
	192	0.164	0.258	0.195	0.308	0.222	0.334	0.313	0.413	0.296	0.386	0.266	0.368	0.348	0.433
	336	0.188	0.283	0.212	0.313	0.231	0.338	0.290	0.381	0.300	0.394	0.280	0.380	0.350	0.433
	720	0.236	0.332	0.231	0.343	0.254	0.361	0.262	0.344	0.373	0.439	0.283	0.376	0.340	0.420
Exchange	96	0.079	0.204	0.139	0.276	0.197	0.323	1.292	0.849	0.847	0.752	0.968	0.812	1.065	0.829
	192	0.159	0.292	0.256	0.369	0.300	0.369	1.631	0.968	1.204	0.895	1.040	0.851	1.188	0.906
	336	0.270	0.398	0.426	0.464	0.509	0.524	2.225	1.145	1.672	1.036	1.659	1.081	1.357	0.976
	720	0.536	0.574	1.090	0.800	1.447	0.941	2.521	1.245	2.478	1.310	1.941	1.127	1.510	1.016
Traffic	96	0.416	0.294	0.562	0.349	0.613	0.388	0.824	0.514	0.719	0.391	0.684	0.384	0.732	0.423
	192	0.408	0.288	0.562	0.346	0.616	0.382	1.106	0.672	0.696	0.379	0.685	0.390	0.733	0.420
	336	0.425	0.298	0.570	0.323	0.622	0.337	1.084	0.627	0.777	0.420	0.733	0.408	0.742	0.420
	720	0.520	0.353	0.596	0.368	0.660	0.408	1.536	0.845	0.864	0.472	0.717	0.396	0.755	0.423
Weather	96	0.199	0.262	0.217	0.296	0.266	0.336	0.406	0.444	0.300	0.384	0.458	0.490	0.689	0.596
	192	0.228	0.288	0.276	0.336	0.307	0.367	0.525	0.527	0.598	0.544	0.658	0.589	0.752	0.638
	336	0.267	0.323	0.339	0.380	0.359	0.395	0.531	0.539	0.578	0.523	0.797	0.652	0.639	0.596
	720	0.319	0.361	0.403	0.428	0.578	0.578	0.419	0.428	1.059	0.741	0.869	0.675	1.130	0.792
ILI	24	1.970	0.875	2.203	0.963	3.483	1.287	4.631	1.484	5.764	1.677	4.480	1.444	4.400	1.382
	36	1.982	0.859	2.272	0.976	3.103	1.148	4.123	1.348	4.755	1.467	4.799	1.467	4.783	1.448
	48	1.868	0.896	2.209	0.981	2.669	1.085	4.066	1.36	4.763	1.469	4.800	1.468	4.832	1.465
	60	2.057	0.929	2.545	1.061	2.770	1.125	4.278	1.41	5.264	1.564	5.278	1.560	4.882	1.483

To evaluate the proposed FiLM, we conduct extensive experiments on six popular real-world benchmark datasets for long-term forecasting, including traffic, energy, economics, weather, and disease. Since classic models such as ARIMA and simple RNN/TCN models perform inferior as shown in Zhou et al. (2021) and Wu et al. (2021), we mainly include five state-of-the-art (SOTA) Transformer-based models, i.e., FEDformer, Autoformer Wu et al. (2021), Informer Zhou et al. (2021), LogTrans Li et al. (2019), Reformer Kitaev et al. (2020), and one recent state-space model with recursive memory S4 Gu et al. (2021a), for comparison. FEDformer is selected as the main baseline as it achieves SOTA results in most settings. More details about baseline models, datasets, and implementations are described in Appendix C.

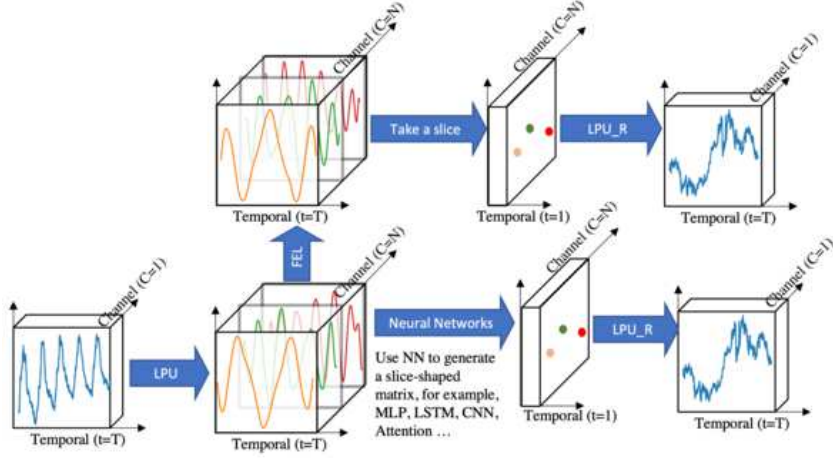


Figure 6: LPU boosting effect. LPU can serve as a plug-in block in various backbones, e.g., FEL, MLP, LSTM, CNN, and Attention. Replacing LPU with a comparable-sized linear layer will always lead to degraded performance.

4.1 Main Result

For better comparison, we follow the experiment settings of Informer Zhou et al. (2021) where the input length is tuned for best forecasting performance, and the prediction lengths for both training and evaluation are fixed to be 96, 192, 336, and 720, respectively.

Multivariate Results In multivariate forecasting tasks, FiLM achieves the best performance on all six benchmark datasets at all horizons, as shown in Table 1. Compared with SOTA work (FEDformer), our proposed FiLM yields an overall **20.3%** relative MSE reduction. It is worth noting that the improvement is even more significant on some of the datasets, such as Exchange (over 30%). The Exchange dataset does not exhibit apparent periodicity, but FiLM still achieves superior performance. The improvements made by FiLM are consistent with varying horizons, demonstrating its strength in long-term forecasting. More results on the ETT full benchmark are provided in Appendix C.5.

Univariate Results The benchmark results for univariate time series forecasting are summarized in Appendix C.4, Table 10. Compared with SOTA work (FEDformer), FiLM yields an overall **22.6%** relative MSE reduction. And on some datasets, such as Weather and Electricity, the improvement can reach more than 40%. It again proves the effectiveness of FiLM in long-term forecasting.

LPU Boosting Results

A set of experiments are conducted to measure the boosting effect of LPU when combined with various common deep learning modules (MLP, LSTM, CNN, and Attention), as shown in Figure 6. In the experiment, we compare the LPU and the comparable-sized linear layer. It is worth mentioning that LPU does not contain any learnable parameter. The results are shown in Table 2. For all the modules, LPU significantly improves their average performance for long-term forecasting: MLP: **119.4%**, LSTM: **97.0%**, CNN: **13.8%**, Attention: **8.2%**. Vanilla Attention has a relative poor performance when combining the LPU, which worth further digging.

Low-rank Approximation for FEL

Low-rank approximation of learnable matrix in Frequency Enhanced Layer

Table 3: Low-rank Approximation (LRA) study for Frequency Enhanced Layer (FEL): Comp. K=0 means default version without LRA, 1 means the largest compression using k=1

Comp. K	0		16		4		1		
Metric	MSE	MAE	MSE	MAE	MSE	MAE	MSE	MAE	
ETTh1	96	0.371	0.394	0.371	0.396	0.371	0.398	0.400	0.421
	192	0.414	0.423	0.411	0.423	0.414	0.426	0.435	0.444
	336	0.442	0.445	0.443	0.446	0.443	0.444	0.492	0.478
	720	0.454	0.451	0.464	0.474	0.468	0.478	0.501	0.499
ETMh1	96	0.199	0.262	0.199	0.263	0.197	0.262	0.198	0.263
	192	0.228	0.288	0.225	0.285	0.226	0.285	0.225	0.286
	336	0.245	0.295	0.242	0.292	0.241	0.292	0.240	0.291
	720	0.262	0.312	0.259	0.310	0.258	0.310	0.257	0.310

can significantly reduce our parameter size to **0.1%~0.4%** with minor accuracy deterioration. The experiment details are shown in Table 3. Compared to Transformer-based baselines, FiLM enjoys **80%** learnable parameter reduction and **50%** memory usage reductions, as shown in Appendix G, H.

Mode selection policy for FEL Frequency mode selection policy is studied in Table 4. The *Lowest* mode selection method shows the most robust performance. The results in *Low random* column shows that randomly adding some high-frequency signal gives extra improvement in some datasets, as our theoretical studies in Theorem 3 support.

4.2 Ablation Study

This subsection presents the ablation study of the two major blocks (FEL & LPU) employed, the multiscale mechanism, and data normalization (RevIN).

Table 5: Ablation studies of LPU layer. The original LPU block (whose projection and reconstruction matrix are fixed) is replaced with 6 variants (**Fixed** means the matrix are not trainable. **Trainable** means the matrix is initialized with original parameters and trainable. **Random Init** means the matrix is initialized randomly and trainable). The experiments are performed on ETTm1 and Electricity with different input lengths. The metric of variants is presented in relative value ('+' indicates degraded performance, '-' indicates improved performance).

Index		Original		Variant 1		Variant 2		Variant 3		Variant 4		Variant 5		Variant 6	
Projection		Fixed						Trainable				Random Init		Linear	
Reconstruction		Fixed		Trainable		Fixed		Trainable		Random Init		-		Linear	
Metric		MSE	MAE	MSE	MAE	MSE	MAE	MSE	MAE	MSE	MAE	-	-	MSE	MAE
ETTm1	96	0.030	0.128	+6.0%	+3.1%	+4.6%	+3.1%	+4.7%	+2.7%	+0.7%	+0.6%	NaN	NaN	+38%	+22%
	192	0.047	0.160	-2.6%	-1.3%	+2.5%	+1.8%	-0.4%	+0.4%	-3.0%	-1.0%	NaN	NaN	+9.5%	+8.7%
	336	0.063	0.185	+4.2%	+1.8%	-2.4%	-0.4%	-6.3%	-2.5%	+2.2%	+1.4%	NaN	NaN	+5.8%	+5.0%
	720	0.081	0.215	-0.4%	-0.6%	+24%	+12%	+11%	+5.9%	NaN	NaN	NaN	NaN	+1.4%	+2.2%
Electricity	96	0.213	0.328	+15%	+6.8%	+11%	+5.2%	+11%	+5.1%	+11%	+4.8%	NaN	NaN	+136%	+58%
	192	0.268	0.373	-4.6%	-3.8%	+7.8%	+3.9%	+6.8%	+3.5%	-5.3%	-3.9%	NaN	NaN	+32%	+16%
	336	0.307	0.417	-4.2%	-5.0%	-3.9%	-6.0%	-7.2%	-8.0%	-8.5%	-9.0%	NaN	NaN	+0.1%	-5.0%
	720	0.321	0.423	+2.9%	+2.8%	+10%	+6.8%	+3.0%	+1.7%	+207%	+85%	NaN	NaN	37%	22%

Ablation of LPU To prove the effectiveness of LPU layer, in Table 5, we compare the original LPU layer with six variants. The LPU layer consists of two sets of matrices (Projection matrices & Reconstruction matrices). Each has three variants: Fixed, Trainable, and Random Init. In Variant 6, we use comparable-sized linear layers to replace the LPU layer. We observe that Variant 6 leads to a 32.5% degradation on average, which confirms the effectiveness of Legendre projection. The projection matrix in LPU is recursively called N times (N is the input length). So if the projection matrix is randomly initialized (Variant 5), the output will face the problem of exponential explosion. If the projection matrix is trainable (Variants 2, 3, 4), the model suffers from the exponential explosion as well and thus needs to be trained with a small learning rate, which leads to a plodding training speed and requires more epochs for convergence. Thus, the trainable projection version is not recommended, considering the trade-off between speed and performance. The variant with trainable reconstruction matrix (Variant 1) has comparable performance and less difficulty in convergence.

Ablation of FEL To prove the effectiveness of the FEL, we replace the FEL with multiple variants (MLP, LSTM, CNN, and Transformer). S4 is also introduced as a variant since it has a version with Legendre projection memory. The experimental results are summarized in Table 6. FEL achieves the best performance compared with its LSTM, CNN, and Attention counterpart. MLP has comparable

Table 4: Mode selection policy study for frequency enhanced layer: Lowest: select the lowest m frequency mode, random: select M random frequency mode. 3. low random: select the 0.8*M lowest frequency mode and 0.2*M random high frequency mode.

Policy	Lowest		Random		Low random		
	Metric	MSE	MAE	MSE	MAE	MSE	MAE
Exchange	96	0.079	0.204	0.083	0.208	0.087	0.210
	192	0.159	0.292	0.187	0.318	0.207	0.340
	336	0.270	0.398	0.271	0.395	0.353	0.461
	720	0.788	0.680	0.788	0.680	0.748	0.674
Weather	96	0.199	0.262	0.197	0.256	0.196	0.254
	192	0.228	0.288	0.234	0.300	0.234	0.301
	336	0.267	0.323	0.266	0.319	0.263	0.316
	720	0.319	0.361	0.317	0.356	0.316	0.354

Table 6: Ablation studies of FEL layer. The FEL layer is replaced with 4 different variants: MLP, LSTM, CNN, and Transformer. S4 is also introduced as a variant. The experiments are performed on ETTm1 and Electricity. The metric of variants is presented in relative value ('+' indicates degraded performance, '-' indicates improved performance).

Methods	FiLM		LPU+MLP		LPU+LSTM		LPU+CNN		LPU+attention		S4		
	Metric	MSE	MAE	MSE	MAE	MSE	MAE	MSE	MAE	MSE	MAE	MSE	MAE
ETTm1	96	0.030	0.128	+14%	+6.6%	+62%	+31%	+286%	+118%	+709%	+166%	—	—
	192	0.047	0.160	+3.8%	+2.2%	+271%	+122%	+116%	+58%	+727%	+136%	—	—
	336	0.063	0.185	-3.7%	-2.1%	+90%	+51%	+94%	+48%	+2524%	+286%	—	—
	720	0.081	0.215	+0.9%	-0.6%	+127%	+65%	+33%	+17%	+5783%	+299%	—	—
Electricity	96	0.213	0.328	+103%	+40%	+37%	+20%	+46%	+23%	+278%	+105%	65%	38%
	192	0.268	0.373	+8.7%	+0.01%	+32%	+14%	+42%	+21%	+249%	+81%	39%	22%
	336	0.307	0.417	-3.7%	-8.5%	+42%	+13%	+17%	+6.0%	+564%	+90%	33%	15%
	720	0.321	0.423	+5.7%	+1.4%	+98%	+36%	+32%	+18%	+2739%	+117%	47%	22%

performance when input length is 192, 336, and 720. However, MLP suffers from insupportable memory usage, which is N^2L (while FEL is N^2). S4 achieves similar results as our LPU+MLP variant. Among all, the LPU+vanilla Attention variant shows the poorest performance.

Table 7: Ablation studies of Normalization and Multiscale. Multiscale use 3 branches with: T , $2T$, and $4T$ as input sequence length. T is the predicted sequence length

Dataset	ETTm2		Electricity		Exchange		Traffic		Weather		Illness		
	Metric	MSE	Relative	MSE	Relative	MSE	Relative	MSE	Relative	MSE	Relative	MSE	Relative
Methods	Original	0.301	+16%	0.195	+4.8%	0.534	+60%	0.528	+19%	0.264	+4.9%	3.55	+80%
	Normalization	0.268	+3.6%	0.199	+6.4%	0.456	+36%	0.656	+48%	0.256	+1.5%	3.36	+70%
	Multiscale	0.259	+0.19%	0.187	+0%	0.335	0%	0.541	+22%	0.253	+0.50%	2.41	+22%
	With both	0.271	+4.7%	0.189	+1.5%	0.398	+19%	0.442	+0%	0.253	+0.4%	1.97	+0%

Ablation of Multiscale and Data Normalization (RevIN) The multiscale module leads to significant improvement on all datasets consistently. However, the data normalization achieves mixed performance, leading to improved performance on Traffic and Illness but a slight improvement on the rest. The Ablation study of RevIN data normalization and the mixture of multiscale experts employed is shown in Table 7.

4.3 Other Studies

Other supplemental studies are provided in Appendix. 1. A parameter sensitivity experiment (in Appendix D) is carried out to discuss the choice of hyperparameter for M and N, where M is the frequency mode number and N is the Legendre Polynomials number. 2. A noise injection experiment (in Appendix E) is conducted to show the robustness of our model. 3. A Kolmogorov-Smirnov (KS) test (in Appendix F) is conducted to discuss the similarity between the output distribution and the input. Our proposed FiLM has the best results on KS test, which supports our motivation in model design. 4. At last, (in Appendix H), we show that FiLM is an efficient model with shorter training time and smaller memory usage compared to baseline models.

5 Discussions and Conclusion

In long-term forecasting, the critical challenge is the trade-off between historical information preservation and noise reduction for accurate and robust forecasting. To address this challenge, we propose a Frequency improved Legendre Memory model, or **FiLM**, to preserve historical information accurately and remove noisy signals. Moreover, we theoretically and empirically prove the effectiveness of the Legendre and Fourier projection employed in our model. Extensive experiments show that the proposed model achieves SOTA accuracy by a significant margin on six benchmark datasets. In particular, we would like to point out that our proposed framework is rather general and can be used as the building block for long-term forecasting in future research. It can be modified for different scenarios. For example, the Legendre Projection Unit can be replaced with other orthogonal functions such as Fourier, Wavelets, Laguerre Polynomials, Chebyshev Polynomials, etc. In addition, based on the properties of noises, Fourier Enhanced Layer is proved to be one of the best candidate in the framework. We plan to investigate more variants of this framework in the future.

References

Box, G. E. P. and Jenkins, G. M. Some recent advances in forecasting and control. *Journal of the Royal Statistical Society. Series C (Applied Statistics)*, 17(2):91–109, 1968.

Box, G. E. P. and Pierce, D. A. Distribution of residual autocorrelations in autoregressive-integrated moving average time series models. volume 65, pp. 1509–1526. Taylor & Francis, 1970.

Choromanski, K. M., Likhoshesterov, V., Dohan, D., Song, X., Gane, A., Sarlós, T., Hawkins, P., Davis, J. Q., Mohiuddin, A., Kaiser, L., Belanger, D. B., Colwell, L. J., and Weller, A. Rethinking attention with performers. In *9th International Conference on Learning Representations (ICLR), Virtual Event, Austria, May 3-7, 2021*, 2021.

Chung, J., Gülcöhre, C., Cho, K., and Bengio, Y. Empirical evaluation of gated recurrent neural networks on sequence modeling. *CoRR*, abs/1412.3555, 2014.

Devlin, J., Chang, M., Lee, K., and Toutanova, K. BERT: pre-training of deep bidirectional transformers for language understanding. In *Proceedings of the 2019 Conference of the North American Chapter of the Association for Computational Linguistics: Human Language Technologies (NAACL-HLT), Minneapolis, MN, USA, June 2-7, 2019*, pp. 4171–4186, 2019.

Dosovitskiy, A., Beyer, L., Kolesnikov, A., Weissenborn, D., Zhai, X., Unterthiner, T., Dehghani, M., Minderer, M., Heigold, G., Gelly, S., Uszkoreit, J., and Houlsby, N. An image is worth 16x16 words: Transformers for image recognition at scale. In *9th International Conference on Learning Representations, ICLR 2021, Virtual Event, Austria, May 3-7, 2021*, 2021.

Gu, A., Dao, T., Ermon, S., Rudra, A., and Ré, C. Hippo: Recurrent memory with optimal polynomial projections. *Advances in Neural Information Processing Systems*, 33:1474–1487, 2020.

Gu, A., Goel, K., and Ré, C. Efficiently modeling long sequences with structured state spaces. *arXiv preprint arXiv:2111.00396*, 2021a.

Gu, A., Johnson, I., Goel, K., Saab, K., Dao, T., Rudra, A., and Ré, C. Combining recurrent, convolutional, and continuous-time models with linear state space layers. *Advances in Neural Information Processing Systems*, 34, 2021b.

Gupta, G., Xiao, X., and Bogdan, P. Multiwavelet-based operator learning for differential equations. In *Advances in Neural Information Processing Systems (NeurIPS), 2021, December 6-14, 2021, virtual*, pp. 24048–24062, 2021.

Hochreiter, S. and Schmidhuber, J. Long short-term memory. *Neural computation*, 9(8):1735–1780, 1997a.

Hochreiter, S. and Schmidhuber, J. Long Short-Term Memory. *Neural Computation*, 9(8):1735–1780, November 1997b. ISSN 0899-7667, 1530-888X.

Kim, T., Kim, J., Tae, Y., Park, C., Choi, J.-H., and Choo, J. Reversible instance normalization for accurate time-series forecasting against distribution shift. In *International Conference on Learning Representations*, 2021.

Kingma, D. P. and Ba, J. Adam: A Method for Stochastic Optimization. *arXiv:1412.6980 [cs]*, January 2017. arXiv: 1412.6980.

Kitaev, N., Kaiser, L., and Levskaya, A. Reformer: The efficient transformer. In *8th International Conference on Learning Representations, ICLR 2020, Addis Ababa, Ethiopia, April 26-30, 2020*, 2020.

Lai, G., Chang, W.-C., Yang, Y., and Liu, H. Modeling long-and short-term temporal patterns with deep neural networks. In *The 41st International ACM SIGIR Conference on Research & Development in Information Retrieval*, pp. 95–104, 2018.

Lee-Thorp, J., Ainslie, J., Eckstein, I., and Ontañón, S. FNet: Mixing tokens with fourier transforms. *CoRR*, abs/2105.03824, 2021.

Li, S., Jin, X., Xuan, Y., Zhou, X., Chen, W., Wang, Y.-X., and Yan, X. Enhancing the locality and breaking the memory bottleneck of transformer on time series forecasting. In *Advances in Neural Information Processing Systems*, volume 32, 2019.

Li, Z., Kovachki, N. B., Azizzadenesheli, K., Liu, B., Bhattacharya, K., Stuart, A. M., and Anandkumar, A. Fourier neural operator for parametric partial differential equations. *CoRR*, abs/2010.08895, 2020.

Ma, X., Kong, X., Wang, S., Zhou, C., May, J., Ma, H., and Zettlemoyer, L. Luna: Linear unified nested attention. *CoRR*, abs/2106.01540, 2021.

Pascanu, R., Mikolov, T., and Bengio, Y. On the difficulty of training recurrent neural networks. In *Proceedings of the 30th International Conference on Machine Learning, ICML 2013, Atlanta, GA, USA, 16-21 June 2013*, volume 28, pp. 1310–1318, 2013.

Paszke, A., Gross, S., Massa, F., Lerer, A., Bradbury, J., Chanan, G., Killeen, T., Lin, Z., Gimelshein, N., Antiga, L., Desmaison, A., Kopf, A., Yang, E., DeVito, Z., Raison, M., Tejani, A., Chilamkurthy, S., Steiner, B., Fang, L., Bai, J., and Chintala, S. Pytorch: An imperative style, high-performance deep learning library. In *Advances in Neural Information Processing Systems*, pp. 8024–8035. 2019.

Qin, Y., Song, D., Chen, H., Cheng, W., Jiang, G., and Cottrell, G. W. A dual-stage attention-based recurrent neural network for time series prediction. In *Proceedings of the Twenty-Sixth International Joint Conference on Artificial Intelligence (IJCAI), Melbourne, Australia, August 19-25, 2017*, pp. 2627–2633. ijcai.org, 2017.

Qiu, J., Ma, H., Levy, O., Yih, W., Wang, S., and Tang, J. Blockwise self-attention for long document understanding. In *Findings of the Association for Computational Linguistics: EMNLP 2020, Online Event, 16-20 November 2020*, volume EMNLP 2020 of *Findings of ACL*, pp. 2555–2565. Association for Computational Linguistics, 2020.

Rangapuram, S. S., Seeger, M. W., Gasthaus, J., Stella, L., Wang, Y., and Januschowski, T. Deep state space models for time series forecasting. In *Advances in Neural Information Processing Systems*, volume 31, 2018.

Rao, Y., Zhao, W., Zhu, Z., Lu, J., and Zhou, J. Global filter networks for image classification. *Advances in Neural Information Processing Systems*, 34, 2021.

Salinas, D., Flunkert, V., Gasthaus, J., and Januschowski, T. DeepAR: Probabilistic forecasting with autoregressive recurrent networks. *International Journal of Forecasting*, 36(3):1181–1191, 2020.

Sen, R., Yu, H., and Dhillon, I. S. Think globally, act locally: A deep neural network approach to high-dimensional time series forecasting. In *Advances in Neural Information Processing Systems (NeurIPS), December 8-14, 2019, Vancouver, BC, Canada*, pp. 4838–4847, 2019.

Tay, Y., Bahri, D., Yang, L., Metzler, D., and Juan, D. Sparse sinkhorn attention. In *Proceedings of the 37th International Conference on Machine Learning, ICML 2020, 13-18 July 2020, Virtual Event*, volume 119 of *Proceedings of Machine Learning Research*, pp. 9438–9447. PMLR, 2020a.

Tay, Y., Dehghani, M., Abnar, S., Shen, Y., Bahri, D., Pham, P., Rao, J., Yang, L., Ruder, S., and Metzler, D. Long range arena: A benchmark for efficient transformers. *arXiv preprint arXiv:2011.04006*, 2020b.

Vaswani, A., Shazeer, N., Parmar, N., Uszkoreit, J., Jones, L., Gomez, A. N., Kaiser, Ł., and Polosukhin, I. Attention is all you need. *Advances in neural information processing systems*, 30, 2017.

Voelker, A., Kajić, I., and Eliasmith, C. Legendre memory units: Continuous-time representation in recurrent neural networks. In *Advances in Neural Information Processing Systems*, volume 32, 2019.

Wang, J., Wang, Z., Li, J., and Wu, J. Multilevel wavelet decomposition network for interpretable time series analysis. In *Proceedings of the 24th ACM SIGKDD International Conference on Knowledge Discovery & Data Mining*, pp. 2437–2446, 2018.

Wang, S., Li, B. Z., Khabsa, M., Fang, H., and Ma, H. Linformer: Self-attention with linear complexity. *CoRR*, abs/2006.04768, 2020.

Wen, Q., Zhou, T., Zhang, C., Chen, W., Ma, Z., Yan, J., and Sun, L. Transformers in time series: A survey. *arXiv preprint arXiv:2202.07125*, 2022.

Wu, H., Xu, J., Wang, J., and Long, M. Autoformer: Decomposition transformers with auto-correlation for long-term series forecasting. In *Proceedings of the Advances in Neural Information Processing Systems (NeurIPS)*, pp. 101–112, 2021.

Xiong, Y., Zeng, Z., Chakraborty, R., Tan, M., Fung, G., Li, Y., and Singh, V. Nyströmformer: A nyström-based algorithm for approximating self-attention. In *Thirty-Fifth AAAI Conference on Artificial Intelligence*, pp. 14138–14148, 2021.

Zhang, J., Lin, Y., Song, Z., and Dhillon, I. S. Learning long term dependencies via fourier recurrent units. In *Proceedings of the 35th International Conference on Machine Learning (ICML), Stockholmsmässan, Stockholm, Sweden, July 10-15, 2018*, volume 80, pp. 5810–5818, 2018.

Zhou, H., Zhang, S., Peng, J., Zhang, S., Li, J., Xiong, H., and Zhang, W. Informer: Beyond efficient transformer for long sequence time-series forecasting. In *The Thirty-Fifth AAAI Conference on Artificial Intelligence, AAAI 2021, Virtual Conference*, volume 35, pp. 11106–11115, 2021.

Zhou, T., Ma, Z., Wen, Q., Wang, X., Sun, L., and Jin, R. FEDformer: Frequency enhanced decomposed transformer for long-term series forecasting. In *39th International Conference on Machine Learning (ICML)*, 2022.

Zhu, Z. and Soricut, R. H-transformer-1d: Fast one-dimensional hierarchical attention for sequences. In *Proceedings of the 59th Annual Meeting of the Association for Computational Linguistics (ACL) 2021, Virtual Event, August 1-6, 2021*, pp. 3801–3815, 2021.

Checklist

A Related Work

In this section, an overview of the literature for time series forecasting will be given.

Traditional Time Series Models The first generation of well-discussed time series model is the autoregressive family. ARIMA [Box & Jenkins \(1968\)](#); [Box & Pierce \(1970\)](#) follows the Markov process and build recursive sequential forecasting. However, an autoregressive process has difficulty in dealing non-stationary sequences. Thus, ARIMA employed a pre-process iteration by differencing, which transforms the series to stationary.

Deep Neural Network in Forecasting With the bloom of deep neural networks, recurrent neural networks (RNN) was designed for tasks involving sequential data. However, canonical RNN tends to suffer from gradient vanishing/exploding problem with long input because of its recurrent structure. Among the family of RNNs, LSTM [Hochreiter & Schmidhuber \(1997b\)](#) and GRU [Chung et al. \(2014\)](#) proposed gated structure to control the information flow to deal with the gradient vanishing/exploration problem. Although recurrent networks enjoys fast inference, they are slow to train and not parallelizable. Temporal convolutional network (TCN) [Sen et al. \(2019\)](#) is another family for sequential tasks. However, limited to the reception field of the kernel, the long-term dependencies are hard to grasp. Convolution is a parallelizable operation but expensive in inference.

Efficient Transformers With the innovation of transformers in natural language processing [Vaswani et al. \(2017\)](#); [Devlin et al. \(2019\)](#) and computer vision tasks [Dosovitskiy et al. \(2021\)](#); [Rao et al. \(2021\)](#), transformer-based models are also discussed, renovated, and applied in time series forecasting [Zhou et al. \(2021\)](#); [Wu et al. \(2021\)](#). Some works use temporal attention [Qin et al. \(2017\)](#) to capture long-range dependencies. Others use the backbone of Transformer. Transformers usually employs an encoder-decoder architecture, with the self-attention and cross-attention mechanisms serving as the core layers. However, when employing a point-wise connected attention mechanism, the transformers suffer from quadratic computation complexity.

To get efficient computation without sacrificing too much on performance, the earliest modifications specify the attention matrix with predefined patterns. Examples include: [Qiu et al. \(2020\)](#) uses block-wise attention which reduces the complexity to the square of block size. LogTrans [Li et al. \(2019\)](#) uses log-sparse attention and achieves $N \log^2 N$ complexity. H-transformer [Zhu & Soricut \(2021\)](#) uses a hierarchical pattern for sparse approximation of attention matrix with $O(n)$ complexity. Another strategy is to use dynamic patterns: Reformer [Kitaev et al. \(2020\)](#) introduces a local-sensitive hashing which reduces the complexity to $N \log N$. [Zhu & Soricut \(2021\)](#) introduces a hierarchical pattern. Sinkhorn [Tay et al. \(2020a\)](#) employs a block sorting method to achieve quasi-global attention with only local windows.

Similarly, some work employs a top-k truncating to accelerate computing: Informer [Zhou et al. \(2021\)](#) uses a KL-divergence based method to select top-k in attention matrix. This sparser matrix costs only $N \log N$ in complexity. Autoformer [Wu et al. \(2021\)](#) introduces an auto-correlation block in place of canonical attention to get the sub-series level attention, which achieves $N \log N$ complexity.

Another emerging strategy is to employ a low-rank approximation of the attention matrix. Linformer [Wang et al. \(2020\)](#) uses trainable linear projection to compress the sequence length and achieves $O(n)$ complexity and theoretically proves the boundary of approximation error based on JL lemma. Luna [Ma et al. \(2021\)](#) develops a nested linear structure with $O(n)$ complexity. Nyströmformer [Xiong et al. \(2021\)](#) leverages the idea of Nyström approximation in the attention mechanism and achieves an $O(n)$ complexity. Performer [Choromanski et al. \(2021\)](#) adopts an orthogonal random features approach to efficiently model kernelizable attention mechanisms.

Orthogonal Basis and Neural Network Orthogonal basis project arbitrary functions onto a certain space and thus enable the representation learning in another view. Orthogonal basis family is easy to be discretized and to serve as an plug-in operation in neural networks. Recent studies began to realize the efficiency and effectiveness of Orthogonal basis, including the polynomial family and others (Fourier basis & Multiwavelet basis). Fourier basis is first introduced for acceleration due to Fast Fourier algorithm, for example, acceleration of computing convolution [Gu et al. \(2020\)](#) or Auto-correlation function [Wu et al. \(2021\)](#). Fourier basis also serves as a performance boosting block:

Fourier with Recurrent structure [Zhang et al. \(2018\)](#), Fourier with MLP [Li et al. \(2020\)](#); Lee-Thorp [et al. \(2021\)](#) and Fourier in Transformer [Zhou et al. \(2022\)](#). Multiwavelet transform is a more local filter (compared with Fourier) and a frequency decomposer. Thus, neural networks which employ multiwavelet filter usually exhibit a hierarchical structure and treat different frequency in different tunnels, for example, [Wang et al. \(2018\)](#); [Gupta et al. \(2021\)](#); [Zhou et al. \(2022\)](#). Orthogonal Polynomials are naturally good selections of orthogonal basis. Legendre Memory Unit (LMU) [Voelker et al. \(2019\)](#) uses Legendre Polynomials for an orthogonal projection of input signals for a memory strengthening with the backbone of LSTM. The projection process is mathematically derived from delayed linear transfer function. HiPPO [Gu et al. \(2020\)](#), based on LMU, proposes a novel mechanism (Scaled Legendre), which involves the function’s full history (LMU uses rolling windowed history). In the subsequent work of HiPPO, the authors propose S4 [Gu et al. \(2021a\)](#) model and gives the first practice on time series forecasting tasks. However, LMU and HiPPO shared the same backbone (LSTM), which may limit their performance.

B Algorithm Implementation

Algorithm 1 Frequency Enhanced Layer

```

class Freq_enhanced_layer(nn.Module):
    def __init__(self, in_channels, out_channels, modes1, compression=0):
        super(Freq_enhanced_layer, self).__init__()
        self.in_channels = in_channels
        self.out_channels = out_channels
        self.modes1 = modes1 #Number of Fourier modes to multiply, at most floor(N/2) + 1
        self.compression= compression
        self.scale = (1 / (in_channels*out_channels))
        self.weights1 = nn.Parameter(self.scale * torch.rand(in_channels, out_channels, self.modes1))
        if compression>0: ## Low-rank approximation
            self.weights0 = nn.Parameter(self.scale * torch.rand(in_channels, self.compression, dtype=
                torch.cfloat))
            self.weights1 = nn.Parameter(self.scale * torch.rand(self.compression, self.compression, len(
                self.index), dtype=torch.cfloat))
            self.weights2 = nn.Parameter(self.scale * torch.rand(self.compression, out_channels, dtype=
                torch.cfloat))

    def forward(self, x):
        B, H, E, N = x.shape
        # Compute Fourier coefficients up to factor of e^(- something constant)
        x_ft = torch.fft.rfft(x)
        # Multiply relevant Fourier modes
        out_ft = torch.zeros(B,H, self.out_channels, x.size(-1)//2 + 1)
        if self.compression==0:
            a = x_ft[:, :, :, :self.modes1]
            out_ft[:, :, :, :self.modes1] = torch.einsum("bjix,iox->bjox", a, self.weights1)
        else:
            a = x_ft[:, :, :, :self.modes2]
            a = torch.einsum("bjix,ih->bjhx", a, self.weights0)
            a = torch.einsum("bjhx,hkx->bjxk", a, self.weights1)
            out_ft[:, :, :, :self.modes2] = torch.einsum("bjxk,ko->bjox", a, self.weights2)
        # Return to physical space
        x = torch.fft.irfft(out_ft, n=x.size(-1))
        return x

```

C Dataset and Implementation Details

C.1 Dataset Details

In this paragraph, the details of the experiment datasets are summarized as follows: 1) ETT [Zhou et al. \(2021\)](#) dataset contains two sub-dataset: ETT1 and ETT2, collected from two electricity transformers. Each of them has two versions with different resolutions (15min & 1h). ETT dataset contains multiple series of loads and one series of oil temperatures. 2) Electricity¹ dataset contains the electricity consumption of clients with each column corresponding to one client. 3) Exchange [Lai et al. \(2018\)](#) dataset contains the current exchange of 8 countries. 4) Traffic² dataset contains the occupation rate of freeway system across the State of California. 5) Weather³ dataset contains 21

¹<https://archive.ics.uci.edu/ml/datasets/ElectricityLoadDiagrams 20112014>

²<http://pems.dot.ca.gov>

³<https://www.bgc-jena.mpg.de/wetter/>

Algorithm 2 LPU layer

```
from scipy import signal
from scipy import special as ss
class LPU(nn.Module):
    def __init__(self, N=256, dt=1.0, discretization='bilinear'):
        # N: the order of the Legendre projection
        # dt: step size - can be roughly inverse to the length of the sequence
        super(LPU, self).__init__()
        self.N = N
        A, B = transition(N) ### LMU projection matrix
        A, B, _, _, _ = signal.cont2discrete((A, B, C, D), dt=dt, method=discretization)
        B = B.squeeze(-1)
        self.register_buffer('A', torch.Tensor(A))
        self.register_buffer('B', torch.Tensor(B))
    def forward(self, inputs):
        # inputs: (length, ...)
        # output: (length, ..., N) where N is the order of the Legendre projection
        c = torch.zeros(inputs.shape[:-1] + tuple([self.N]))
        cs = []
        for f in inputs.permute([-1, 0, 1]):
            f = f.unsqueeze(-1)
            new = f @ self.B.unsqueeze(0) # [B, D, H, 256]
            c = F.linear(c, self.A) + new
            cs.append(c)
        return torch.stack(cs, dim=0)
    def reconstruct(self, c):
        a = (self.eval_matrix @ c.unsqueeze(-1)).squeeze(-1)
        return (self.eval_matrix @ c.unsqueeze(-1)).squeeze(-1)
```

Table 8: Summarized feature details of six datasets.

DATASET	LEN	DIM	FREQ
ETTM2	69680	8	15 MIN
ELECTRICITY	26304	322	1H
EXCHANGE	7588	9	1 DAY
TRAFFIC	17544	863	1H
WEATHER	52696	22	10 MIN
ILI	966	8	7 DAYS

meteorological indicators for a range of 1 year in Germany. 6) Illness⁴ dataset contains the influenza-like illness patients in the United States. Table 8 summarizes feature details (Sequence Length: Len, Dimension: Dim, Frequency: Freq) of the six datasets. All datasets are split into the training set, validation set and test set by the ratio of 7:1:2.

C.2 Implementation Details

Our model is trained using ADAM Kingma & Ba (2017) optimizer with a learning rate of $1e^{-4}$. The batch size is set to 32 (In fact, a batch size up to 256 will not deteriorate the performance but with faster training speed). An early stopping counter is employed to stop the training process after three epochs if no loss degradation on the valid set is observed. The mean square error (MSE) and mean absolute error (MAE) are used as metrics. All experiments are repeated 5 times and the mean of the metrics is used in the final results. All the deep learning networks are implemented in PyTorch Paszke et al. (2019) and trained on NVIDIA V100 32GB GPUs.

C.3 Experiments Error Bars

We train our model 5 times and calculate the error bars for FiLM and SOTA model FEDformer to show the robustness of our proposed model.

C.4 Univariate Forecasting Result Table

The univariate benchmark is shown in Table 10.

⁴<https://gis.cdc.gov/grasp/fluvview/fluportaldashboard.html>

Table 9: MSE with error bars (Mean and STD) for FiLM and FEDformer baseline for multivariate long-term forecasting.

	MSE	ETTm2	Electricity	Exchange	Traffic
FiLM	96	0.165 ± 0.0051	0.153 ± 0.0014	0.079 ± 0.002	0.416 ± 0.010
	192	0.222 ± 0.0038	0.165 ± 0.0023	0.159 ± 0.011	0.408 ± 0.007
	336	0.277 ± 0.0021	0.186 ± 0.0018	0.270 ± 0.018	0.425 ± 0.007
	720	0.371 ± 0.0066	0.236 ± 0.0022	0.536 ± 0.026	0.520 ± 0.003
FED-f	96	0.203 ± 0.0042	0.194 ± 0.0008	0.148 ± 0.002	0.217 ± 0.008
	192	0.269 ± 0.0023	0.201 ± 0.0015	0.270 ± 0.008	0.604 ± 0.004
	336	0.325 ± 0.0015	0.215 ± 0.0018	0.460 ± 0.016	0.621 ± 0.006
	720	0.421 ± 0.0038	0.246 ± 0.0020	1.195 ± 0.026	0.626 ± 0.003

Table 10: Univariate long-term series forecasting results on six datasets with input length $I = 96$ and prediction length $O \in \{96, 192, 336, 720\}$. A lower MSE indicates better performance. All experiments are repeated 5 times.

Methods	FiLM		FEDformer		Autoformer		S4		Informer		LogTrans		Reformer		
	Metric	MSE	MAE	MSE	MAE	MSE	MAE	MSE	MAE	MSE	MAE	MSE	MAE	MSE	MAE
ETTm2	96	0.065	0.189	0.063	0.189	0.065	0.189	0.153	0.318	0.088	0.225	0.075	0.208	0.076	0.214
	192	0.094	0.233	0.102	0.245	0.118	0.256	0.183	0.350	0.132	0.283	0.129	0.275	0.132	0.290
	336	0.124	0.274	0.130	0.279	0.154	0.305	0.204	0.367	0.180	0.336	0.154	0.302	0.160	0.312
	720	0.173	0.323	0.178	0.325	0.182	0.335	0.482	0.567	0.300	0.435	0.160	0.321	0.168	0.335
Electricity	96	0.154	0.247	0.253	0.370	0.341	0.438	0.351	0.452	0.484	0.538	0.288	0.393	0.274	0.379
	192	0.166	0.258	0.282	0.386	0.345	0.428	0.373	0.455	0.557	0.558	0.432	0.483	0.304	0.402
	336	0.188	0.283	0.346	0.431	0.406	0.470	0.408	0.477	0.636	0.613	0.430	0.483	0.370	0.448
	720	0.249	0.341	0.422	0.484	0.565	0.581	0.472	0.517	0.819	0.682	0.491	0.531	0.460	0.511
Exchange	96	0.110	0.259	0.131	0.284	0.241	0.387	0.344	0.482	0.591	0.615	0.237	0.377	0.298	0.444
	192	0.207	0.352	0.277	0.420	0.300	0.369	0.362	0.494	1.183	0.912	0.738	0.619	0.777	0.719
	336	0.327	0.461	0.426	0.511	0.509	0.524	0.499	0.594	1.367	0.984	2.018	1.070	1.832	1.128
	720	0.811	0.708	1.162	0.832	1.260	0.867	0.552	0.614	1.872	1.072	2.405	1.175	1.203	0.956
Traffic	96	0.144	0.215	0.170	0.263	0.246	0.346	0.194	0.290	0.257	0.353	0.226	0.317	0.313	0.383
	192	0.120	0.199	0.173	0.265	0.266	0.370	0.172	0.272	0.299	0.376	0.314	0.408	0.386	0.453
	336	0.128	0.212	0.178	0.266	0.263	0.371	0.178	0.278	0.312	0.387	0.387	0.453	0.423	0.468
	720	0.153	0.252	0.187	0.286	0.269	0.372	0.263	0.386	0.366	0.436	0.491	0.437	0.378	0.433
Weather	96	0.0012	0.026	0.0035	0.046	0.011	0.081	0.0061	0.065	0.0038	0.044	0.0046	0.052	0.012	0.087
	192	0.0014	0.029	0.0054	0.059	0.0075	0.067	0.0067	0.067	0.0023	0.040	0.0056	0.060	0.0098	0.079
	336	0.0015	0.030	0.0041	0.050	0.0063	0.062	0.0025	0.0381	0.0041	0.049	0.0060	0.054	0.0050	0.059
	720	0.0022	0.037	0.015	0.091	0.0085	0.070	0.0074	0.0736	0.0031	0.042	0.0071	0.063	0.0041	0.049
LLI	24	0.629	0.538	0.693	0.629	0.948	0.732	0.866	0.584	5.282	2.050	3.607	1.662	3.838	1.720
	36	0.444	0.481	0.554	0.604	0.634	0.650	0.622	0.532	4.554	1.916	2.407	1.363	2.934	1.520
	48	0.557	0.584	0.699	0.696	0.791	0.752	0.813	0.679	4.273	1.846	3.106	1.575	3.754	1.749
	60	0.641	0.644	0.828	0.770	0.874	0.797	0.931	0.747	5.214	2.057	3.698	1.733	4.162	1.847

C.5 ETT Full Benchmark

We present the full-benchmark on the four ETT datasets Zhou et al. (2021) in Table 11 (multivariate forecasting) and Table 12 (univariate forecasting). The ETTh1 and ETTh2 are recorded hourly while ETTm1 and ETTm2 are recorded every 15 minutes. The time series in ETTh1 and ETTm1 follow the same pattern, and the only difference is the sampling rate, similarly for ETTh2 and ETTm2. On average, our FiLM yields a **14.0%** relative MSE reduction for multivariate forecasting, and a **16.8%** reduction for univariate forecasting over the SOTA results from FEDformer.

D Parameter Sensitivity

Influence of legendre functon number N and frequency model number M The experiment results on three different dataset (ETTm1, Electricity, and Exchange) in Figure 7 shows the optimal choice of Legendre Polynomials number (N) when we aim to minimize the reconstruction error (in MSE) for the historical data. The MSE error decreases sharply at first and saturates at an optimal point, where N is in proportion to the input length. For 192, 336, and 720 input sequence, $N \approx 40$, 60, and 100 gives the minimal MSE respectively.

Figure 8 shows the MSE error of time series forecasting on Electricity dataset, with different Legendre Polynomials number (N), mode number and input length. We observe that, when enlarging N, the model performance increases at first and saturates at a point. For example, in Figure 8 Left (input length=192), the best performance is reached when N is larger than 64. While in Figure 8 Right (input length=720), the best performance is reached when N is larger than 128. Another influential parameter is the modes number. From Figure 8 we observe that a small mode number module works as a denoising filter.

Table 11: Multivariate long sequence time-series forecasting results on ETT full benchmark. The best results are highlighted in bold.

Methods	FiLM		FEDformer		Autoformer		S4		Informer		LogTrans		Reformer		
Metric	MSE	MAE	MSE	MAE	MSE	MAE	MSE	MAE	MSE	MAE	MSE	MAE	MSE	MAE	
<i>ETT_{h1}</i>	96	0.371	0.394	0.376	0.419	0.449	0.459	0.949	0.777	0.865	0.713	0.878	0.740	0.837	0.728
	192	0.414	0.423	0.420	0.448	0.500	0.482	0.882	0.745	1.008	0.792	1.037	0.824	0.923	0.766
	336	0.442	0.445	0.459	0.465	0.521	0.496	0.965	0.75	1.107	0.809	1.238	0.932	1.097	0.835
	720	0.465	0.472	0.506	0.507	0.514	0.512	1.074	0.814	1.181	0.865	1.135	0.852	1.257	0.889
<i>ETT_{h2}</i>	96	0.284	0.348	0.346	0.388	0.358	0.397	1.551	0.968	3.755	1.525	2.116	1.197	2.626	1.317
	192	0.357	0.400	0.429	0.439	0.456	0.452	2.336	1.229	5.602	1.931	4.315	1.635	11.12	2.979
	336	0.377	0.417	0.482	0.480	0.482	0.486	2.801	1.259	4.721	1.835	1.124	1.604	9.323	2.769
	720	0.439	0.456	0.463	0.474	0.515	0.511	2.973	1.333	3.647	1.625	3.188	1.540	3.874	1.697
<i>ETT_{m1}</i>	96	0.302	0.345	0.378	0.418	0.505	0.475	0.640	0.584	0.672	0.571	0.600	0.546	0.538	0.528
	192	0.338	0.368	0.426	0.441	0.553	0.496	0.570	0.555	0.795	0.669	0.837	0.700	0.658	0.592
	336	0.373	0.388	0.445	0.459	0.621	0.537	0.795	0.691	1.212	0.871	1.124	0.832	0.898	0.721
	720	0.420	0.420	0.543	0.490	0.671	0.561	0.738	0.655	1.166	0.823	1.153	0.820	1.102	0.841
<i>ETT_{m2}</i>	96	0.165	0.256	0.203	0.287	0.255	0.339	0.705	0.690	0.365	0.453	0.768	0.642	0.658	0.619
	192	0.240	0.313	0.269	0.328	0.281	0.340	0.924	0.692	0.533	0.563	0.989	0.757	1.078	0.827
	336	0.286	0.345	0.325	0.366	0.339	0.372	1.364	0.877	1.363	0.887	1.334	0.872	1.549	0.972
	720	0.393	0.422	0.421	0.415	0.422	0.419	2.074	1.074	3.379	1.338	3.048	1.328	2.631	1.242

Table 12: Univariate long sequence time-series forecasting results on ETT full benchmark. The best results are highlighted in bold.

Methods	FiLM		FEDformer		Autoformer		S4		Informer		LogTrans		Reformer		
Metric	MSE	MAE	MSE	MAE	MSE	MAE	MSE	MAE	MSE	MAE	MSE	MAE	MSE	MAE	
<i>ETT_{h1}</i>	96	0.055	0.178	0.079	0.215	0.071	0.206	0.316	0.490	0.193	0.377	0.283	0.468	0.532	0.569
	192	0.072	0.207	0.104	0.245	0.114	0.262	0.345	0.516	0.217	0.395	0.234	0.409	0.568	0.575
	336	0.083	0.229	0.119	0.270	0.107	0.258	0.825	0.846	0.202	0.381	0.386	0.546	0.635	0.589
	720	0.090	0.240	0.127	0.280	0.126	0.283	0.190	0.355	0.183	0.355	0.475	0.628	0.762	0.666
<i>ETT_{h2}</i>	96	0.127	0.272	0.128	0.271	0.153	0.306	0.381	0.501	0.213	0.373	0.217	0.379	1.411	0.838
	192	0.182	0.335	0.185	0.330	0.204	0.351	0.332	0.458	0.227	0.387	0.281	0.429	5.658	1.671
	336	0.204	0.367	0.231	0.378	0.246	0.389	0.655	0.670	0.242	0.401	0.293	0.437	4.777	1.582
	720	0.241	0.396	0.278	0.420	0.268	0.409	0.630	0.662	0.291	0.439	0.218	0.387	2.042	1.039
<i>ETT_{m1}</i>	96	0.029	0.127	0.033	0.140	0.056	0.183	0.651	0.733	0.109	0.277	0.049	0.171	0.296	0.355
	192	0.041	0.153	0.058	0.186	0.081	0.216	0.190	0.372	0.151	0.310	0.157	0.317	0.429	0.474
	336	0.053	0.175	0.071	0.209	0.076	0.218	0.428	0.581	0.427	0.591	0.289	0.459	0.585	0.583
	720	0.071	0.205	0.102	0.250	0.110	0.267	0.254	0.433	0.438	0.586	0.430	0.579	0.782	0.730
<i>ETT_{m2}</i>	96	0.065	0.189	0.063	0.189	0.065	0.189	0.153	0.318	0.088	0.225	0.075	0.208	0.076	0.214
	192	0.094	0.233	0.102	0.245	0.118	0.256	0.183	0.350	0.132	0.283	0.129	0.275	0.132	0.290
	336	0.124	0.274	0.130	0.279	0.154	0.305	0.204	0.367	0.180	0.336	0.154	0.302	0.160	0.312
	720	0.173	0.323	0.178	0.325	0.182	0.335	0.482	0.567	0.300	0.435	0.160	0.321	0.168	0.335

E Noise Injection Experiment

Our model’s robustness in long-term forecasting tasks can be demonstrated using a series of noise injection experiments as shown in Table 13. As we can see, adding a gaussian noise in the training/test stage have limited effect on our model’s performance, the deterioration is less than 1.5% in the worst case. The model’s robustness is consistent across various of forecasting length. Note that adding the noise in testing stage other than the training stage will even improve our performance by 0.4%, which further supports our claim of robustness .

F Distribution Analysis of Forecasting Output

F.1 Kolmogorov-Smirnov Test

We adopt Kolmogorov-Smirnov (KS) test to check whether the two data samples come from the same distribution. KS test is a nonparametric test of the equality of continuous or discontinuous, two-dimensional probability distributions. In essence, the test answers the question “what is the probability that these two sets of samples were drawn from the same (but unknown) probability distribution”. It quantifies a distance between the empirical distribution function of two samples.

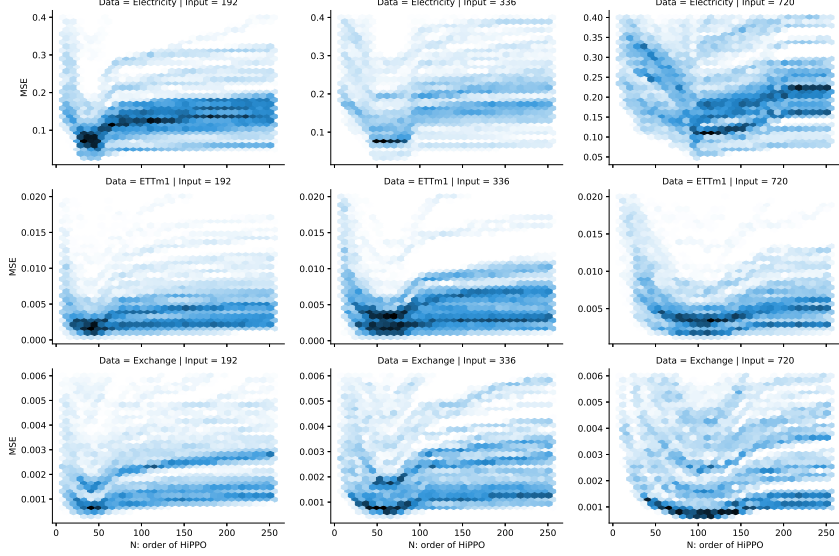


Figure 7: The reconstruction error (MSE) vs order of Legendre Function (N) on three datasets with three different input length.

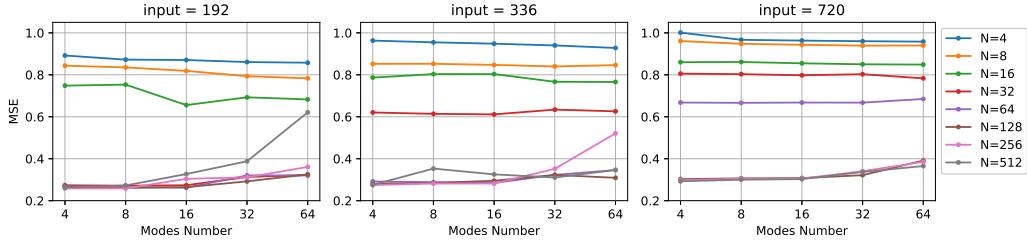


Figure 8: The MSE error of univariate time series forecasting task on Electricity dataset with different Legendre Polynomials number (N), mode number and input length. Left: input length is 192. Mid input length is 336. Right: input length is 720.

The Kolmogorov-Smirnov statistic is

$$D_{n,m} = \sup_x |F_{1,n}(x) - F_{2,m}(x)|$$

where $F_{1,n}$ and $F_{2,m}$ are the empirical distribution functions of the first and the second sample respectively, and \sup is the supremum function. For large samples, the null hypothesis is rejected at level α if

$$D_{n,m} > \sqrt{-\frac{1}{2} \ln \left(\frac{\alpha}{2} \right)} \cdot \sqrt{\frac{n+m}{n \cdot m}},$$

where n and m are the sizes of the first and second samples respectively.

F.2 Distribution Analysis

In this section, we evaluate the distribution similarity between the input sequence and forecasting output of different transformer models quantitatively. In Table 14, we applied the Kolmogorov-Smirnov test to check if the forecasting results of different models made on ETTm1 and ETTm2 are consistent with the input sequences. In particular, we test if the input sequence of fixed 96-time steps come from the same distribution as the predicted sequence, with the null hypothesis that both sequences come from the same distribution. On both datasets, by setting the standard P-value as 0.01, various existing Transformer baseline models have much fewer values than 0.01 except Autoformer, which indicates their forecasting output has a higher probability of being sampled from the different distributions than the input sequence. In contrast, FiLM, Autoformer, and Fedformer have much larger

Table 13: Noise injection studies. A $0.3\mathcal{N}(0, 1)$ gaussian noise is introduced into our training/testing. We conduct 4 sets of experiments with w/wo noise in training and w/wo noise in testing phase. The experiments are performed on ETTm1 and Electricity with different output length. The metric of variants is presented in relative value ('+' indicates degraded performance, '-' indicates improved performance).

Training		without Noise				with Noise			
Testing		WO Noise		W Noise		WO Noise		W Noise	
Metric		MSE	MAE	MSE	MAE	MSE	MAE	MSE	MAE
<i>ETTh1</i>	96	0.371	0.394	-1.6%	-2.0%	-0.0%	-0.0%	-1.6%	-2.0%
	192	0.414	0.423	-0.5%	-1.4%	+0.5%	-0.0%	-0.5%	-1.4%
	336	0.442	0.445	-1.8%	-0.9%	-0.9%	+1.3%	-3.2%	-1.6%
	720	0.465	0.472	+0.2%	-0.2%	+0.9%	+0.9%	-0.6%	-0.4%

Table 14: P-values of Kolmogorov-Smirnov test of different transformer models for long-term forecasting output on ETTm1 and ETTm2 dataset. Larger value indicates the hypothesis (the input sequence and forecasting output come from the same distribution) is less likely to be rejected. The largest results are highlighted.

Methods	Transformer	Informer	Autoformer	FEDformer	FiLM	True	
ETTm1	96	0.0090	0.0055	0.020	0.048	0.016	0.023
	192	0.0052	0.0029	0.015	0.028	0.0123	0.013
	336	0.0022	0.0019	0.012	0.015	0.0046	0.010
	720	0.0023	0.0016	0.008	0.014	0.0024	0.004
ETTm2	96	0.0012	0.0008	0.079	0.071	0.022	0.087
	192	0.0011	0.0006	0.047	0.045	0.020	0.060
	336	0.0005	0.00009	0.027	0.028	0.012	0.042
	720	0.0008	0.0002	0.023	0.021	0.0081	0.023

P-values than others, mainly contributing to their seasonal-trend decomposition mechanism. The proposed FiLM has a much larger P-value than the transformer/informer model. And it's null hypothesis can not be rejected with a P-value larger than 0.01 in all cases of the two datasets. It implies that the output sequence generated by FiLM shares a more similar distribution as the input sequence and thus justifies our design motivation of FiLM as discussed in Section 1. Though FiLM gets a smaller P-value than Fedformer, it is close to the actual output, making a good balance between recovering and forecasting.

G Learnable Parameter Size

Table 15: Parameter size for baseline models and FiLM with different low-rank approximations: the models are trained and tested for ETT dataset. the subscript number is k value for LRA

Methods	Transformer	Autoformer	FEDformer	FiLM	FiLM ₁₆	FiLM ₄	FiLM ₁
Parameter(M)	0.0069	0.0069	0.0098	1.50	0.0293	0.0062	0.00149

Compared to Transformer-based baseline models, FiLM can enjoys a lightweight property with **80%** learnable parameter reductions as shown in Table 15. It has the potential to be used in mobile devices, or, in some situations, require a lightweight model.

H Training Speed and Memory Usage

Memory Usage As shown in Figure 9 (Left), FiLM has a good memory usage with the prolonging output length. For fair comparison, we fix the experimental settings of *Xformer*, where we fix the input length as 96 and prolong the output length. From Figure 9 (Left), we can observe that FiLM has a quasi constant memory usage. Note that the memory usage of FiLM is only linear to input length. Furthermore, FiLM enjoys a much smaller memory usage because of the simple architecture and compressed parameters with low-rank approximation as discussed in G.

Training Speed Experiments are performed on one NVIDIA V100 32GB GPU. As shown in Figure 9 (Right), FiLM has faster training speed with the prolonging output length. For fair comparison, we fix the experimental setting of *Xformer*, where we fix the input length as 96 and prolong the output length. However, in the real experiment settings, we use longer input length (much longer than

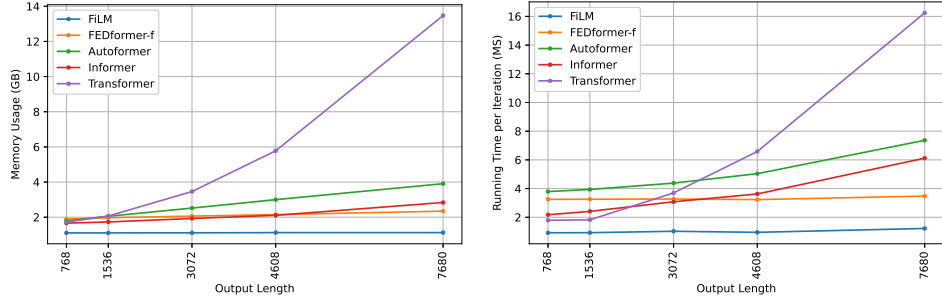


Figure 9: (Left) the memory usage of FiLM and baseline models. (Right) training speed of FiLM and baseline models. The input length is fixed to 96 and the output length is 768, 1536, 3072, 4608, and 7680.

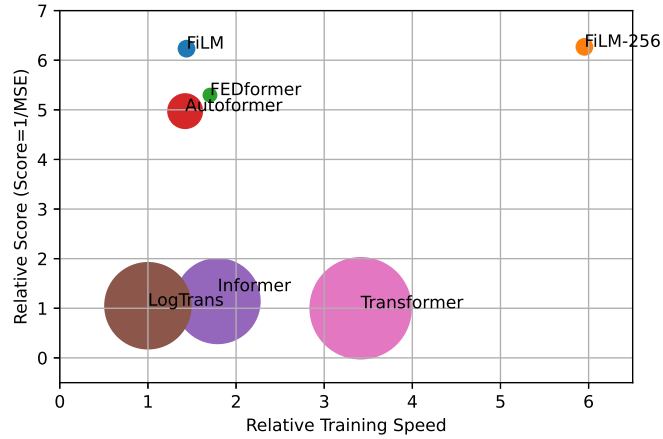


Figure 10: Comparison of training speed and performance of benchmarks. The experiment is performed on ETTm2 with output length = 96, 192, 336, and 720. The performance of the models is measured with *Score*, where $Score = 1/MSE$. Higher *Score* indicates better performance, same for *Speed*. The *Speed* and *Score* is presented on relative value.

96). Thus, the experiment in Figure 9 (Right) is merely a toy case to show the tendency. In Figure 10, we show the average epoch time vs average performance under the settings of benchmarks. The experiment is performed on ETTm2 dataset with output length = 96, 192, 336, and 720. Because of the extreme low memory usage of FiLM, it can be trained with larger batch size (batch size = 256) compared with baselines (batch size = 32). In Figure 10, FiLM-256 exhibits significant advantages on both speed and accuracy. Further more, due to the shallow structure and smaller amount of trainable parameters, FiLM is easy to converge and enjoys smaller performance variation and smaller performance degradation when using large batch size. It worth noting that vanilla Transformer has good training speed because the sequence length not so long. Only a sequence length over one thousand will distinguish the advantage of efficient Transformers.